Journal of Nuclear Materials 390–391 (2009) 452–456

Contents lists available at ScienceDirect

Journal of Nuclear Materials

journal homepage: www.elsevier.com/locate/jnucmat

Edge plasma modelling for transport analysis on JT-60U tokamak

YiPing Chen [a,*], H. Kawashima [b], Xiang Gao [a,1], Liqun Hu [a], N. Asakura [b], K. Shimizu [b], H. Takenaga [b], D.P. Coster [c]

[a] Institute of Plasma Physics, Chinese Academy of Sciences, P.O. Box 1126, Hefei, Anhui, China
[b] Japan Atomic Energy Agency, Naka-Shi, Ibaraki-Ken 311-0193, Japan
[c] Max-Planck-Institut für Plasmaphysik, IPP–EURATOM Association, Boltzmannstrasse 2, D-85748 Garching, Germany

ARTICLE INFO

PACS:
52.25.Fi
52.65.−y
52.40.Hf
52.55.Fa

ABSTRACT

At the edge plasma the cross-field transport is thought to play a major role in determining the shape of density and temperature profiles. The edge plasma transport code B2.5I is used for modelling experimental measurements of the edge plasmas in L-mode and H-mode shots on JT-60U tokamak and the radial transport coefficients at the edge have been obtained by matching the results of the transport code directly to experimental measurements, by which the radial transport coefficients are determined by the combination of the experiment and the transport modelling.

1. Introduction

The anomalous transport plays an important role in the cross-field transport of tokamak plasma. In spite of great progress achieved in tokamak transport theory, the anomalous transport processes are still far from being really understood and an exact estimate of anomalous transport coefficients is very difficult by using present theories. The anomalous transport coefficients from plasma experiment are more reliable, but, in tokamak plasma experiment the anomalous transport coefficients are not directly measured and they depend on the analysis to other experimental data. So, the analysis model and method are key issues for a reasonable determination of anomalous transport coefficients from the experimental measurements. In general, a large-scale plasma transport code includes more realistic physics model and therefore can be used for modelling plasma experiments and deducing anomalous transport coefficients from the experimental data.

B2.5, an important part of SOLPS5.0 code package [1,2], is a two-dimensional edge plasma transport code [1–3] and widely used for modelling tokamak edge plasma. A complete description of the physics model included in the code can be found in [1–3]. More realistic physics models are included in the code, plasma and neutrals are treated by fluid models, the electric potential equation coupled with the fluid equations allows a self-consistent treatment of the electric field. Furthermore, a complete and self-consistent treatment of all classical drifts (including $E \times B$ drifts) and currents naturally arising in the computational region is included as well as a full account of the perpendicular direction [4], which is no more confused with the poloidal direction. Furthermore, atomic and molecular processes, including ionization, recombination, charge exchanges and so on, are taken into account in the code. B2.5I [5,6], which includes experimental data fitting routines based on B2.5, is used for modelling the experimental shots and fitting the experimental data from JT-60U tokamak experimental device [7–9] in order to obtain the anomalous transport coefficients from the experiments. The modelling and fitting are carried out in the edge plasma computation regions, the plasma species include ion, electron and neutrals. The actual MHD equilibrium in the discharges is available. Impurities, drifts and neoclassic transport are not taken into account in present modelling and fitting. The fitted experimental data includes the experimental profiles of plasma temperature and density at the midplane, gas puffing, pumping speed, total particle flux and power flux from the core plasma to the edge computation region, so, the modelling and fitting are based on particle and power balance in the experimental shots. By updating the anomalous transport coefficients in the code and minimizing residuals between the modelling results and the experimental data, finally the anomalous transport coefficients in the shots can be obtained.

2. Edge plasma modelling and the anomalous transport coefficients on JT-60U tokamak

In the present modelling and fitting, only D^0, D^+ and electrons are included in the multi-fluid species of B2.5I. A fluid model is used for neutrals and the drift terms are switched off, the electric

* Corresponding author. Tel.: +86 551 5591368; fax: +86 551 5591310.
E-mail addresses: ypchen@ipp.ac.cn (Y. Chen), xgao@ipp.ac.cn (X. Gao).
[1] Tel.: +86 551 5593108; fax: +86 551 5591310.

0022-3115/$ - see front matter © 2009 Elsevier B.V. All rights reserved.
doi:10.1016/j.jnucmat.2009.01.137

currents and electric field are included in the modelling for all cases. The particle and energy recycling coefficients of the ions to the neutrals are set to 1.0 and 0.3, respectively, at the material boundaries of the computational region. The pumping is set at the inner boundaries of the private flux regions, at the pumping boundaries the particle leakage is $\Gamma_{loss} = \alpha c_s n_a$, c_s is the ion sound speed and n_a is the density of particle species a, $\alpha = 0.01$ for neutrals and $\alpha = 0.001$ for ions, the ions leak off and recycle to the neutrals, the neutrals leak off and are pumped out.

JT-60U is one of the large tokamaks in the world, the main parameters on the device are major radius $R = 3.4$ m, minor radius $a = 1.0$ m, toroidal field $B_t = 4$ T, plasma current $I_p = 3$ MA, plasma volume $V_p = 90$ m^3, pulse length $T_p = 65$ s. Shots 39090 and 37856 on JT-60U tokamak are the deuterium L-mode and H-mode shots, respectively, ohmic and NBI heating are used for the shots. The plasma current I_p, the average electron density n_e and D_α trace versus time in the shots are shown in Fig. 1 and the main parameters in the shots are shown in Table 1. In Table 1, I_p, V_l and B_t are the average plasma current, the loop voltage and the toroidal magnetic field, respectively. R_{axis} is the axis position. P_{OH} and P_{NBI} are the ohmic and NBI heating power, respectively. The total power flux to the computation region is $P = P_{OH} + P_{NBI}$. Φ^{exp}_{pump}, Γ^{exp}_{core} and Γ^{exp}_{puff} are the pumping speed, total particle flux from the core boundary to the computational region and the gas puffing flux, respectively. Although total energy flux from the core boundary to the computational region P can be obtained according to the experimental measurement, for electron and ion energy fluxes to the computational region, P_e and P_i, no exact experiment data is available since a separation of P_e and P_i is not possible in the experiment measurement, so, for the present modelling an assumption that $P_e = P_i = 0.5 \times P$ is made. The ratio P_i/P_e would affect the fitting results of the anomalous transport coefficients. The power in the ion channel usually is larger than in the electron channel when using neutral beams, so, the ratio P_i/P_e may be larger than 1 when NBI is used for heating plasmas, but, how large it is and how it affects the fitting results become two important problems and they should be studied.

For L-mode shot 39090, the computational meshes and the fitting results, the profiles of anomalous particle transport coefficient D and anomalous electron heat transport coefficient χ_e at the midplane are shown in Fig. 2. The computational meshes are orthogonal. Because the profile of ion temperature is not available in the computational region, it is assumed that the anomalous ion heat transport coefficient χ_i and anomalous electron heat transport coefficient χ_e are equal, i.e. $\chi_i = \chi_e$. The fitting results show that the experimental data are well fitted by updating the anomalous particle transport coefficient D and anomalous electron heat transport coefficient χ_e. Fig. 2 shows that D and χ_e increase radially. With these profiles of D and χ_e, the comparison between the modelling results and the experimental measurement is shown in Fig. 3 for the profiles of electron temperature and density at the outer target plate of divertor and for the D_α profile. Although the experimental measurement of plasma density and temperature at the midplane is consistent with the modelling results, for the profiles of plasma density and temperature at the outer target plate a difference between the experimental measurements and the modelling results can be found. So, the good agreement between the experimental measurements and the modelling results at the upstream region is not reproduced in the downstream region and in the target plates of divertor. For the D_α profile, a difference between the experimental measurements and the modelling results can also be found, especially at the inner SOL part. The difference between the experimental measurements and the modelling results for the D_α profile may come from the crude treatment of

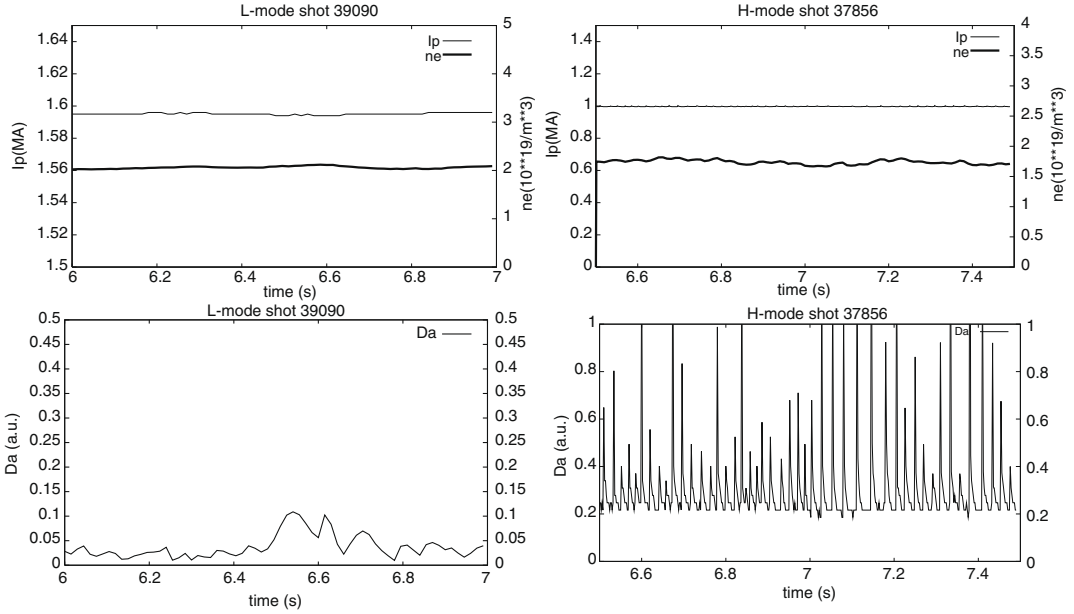

Fig. 1. Plasma current I_p, average electron density n_e and D_α trace versus time in L-mode shot 39090 and H-mode shot 37856.

Table 1
Parameters from JT-60U tokamak shots.

Parameters	Time	R	a	Gas	Mode	I_p	V_l	B_t	R_{axis}	P_{OH}	P_{NBI}	Φ^{exp}_{pump}	Γ^{exp}_{core}	Γ^{exp}_{puff}
Units	s	m	m	–	–	MA	V	T	m	MW	MW	10^{21} s^{-1}	10^{21} s^{-1}	10^{21} s^{-1}
Shot 39090	6.4	3.418	0.970	D_2	L-mode	1.595	0.595	3.116	3.462	0.948	4.500	2.720	0.440	2.280
Shot 37856	7.0	3.433	0.955	D_2	H-mode	0.9971	0.153	1.950	3.527	0.153	5.6	3.021	0.549	2.472

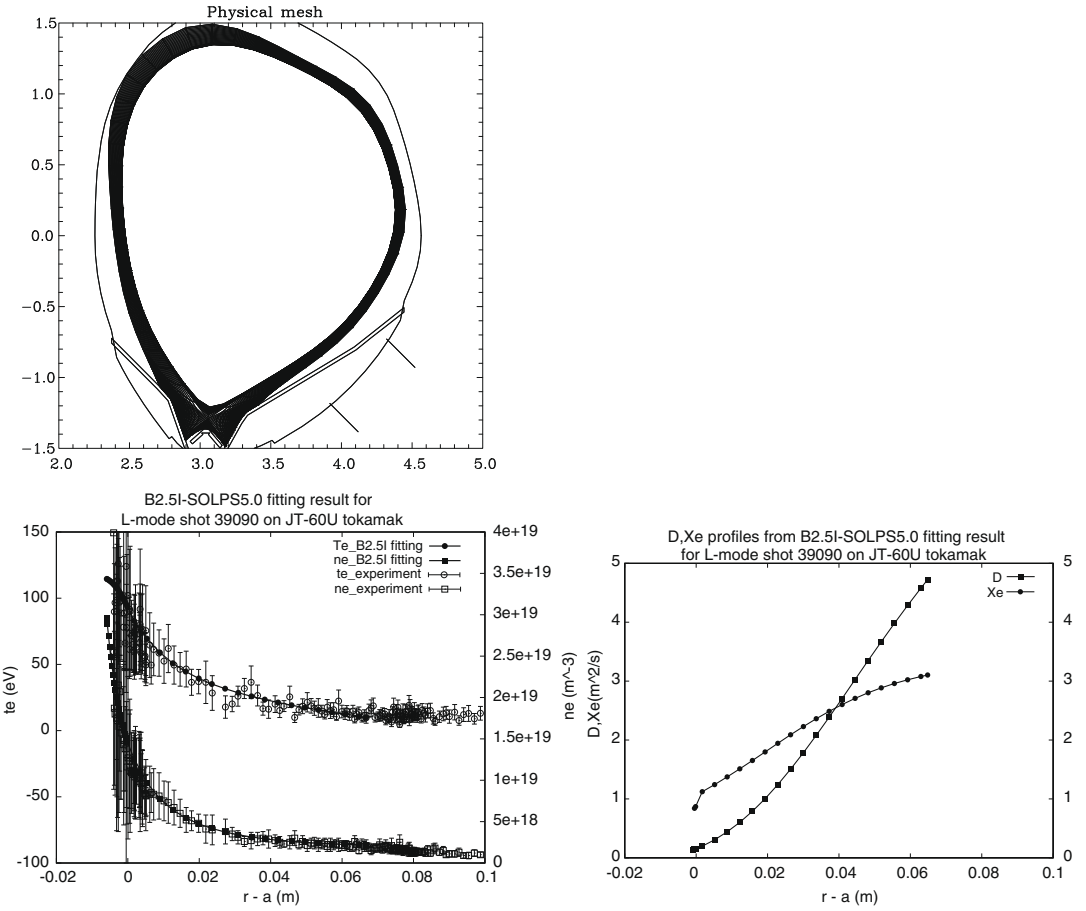

Fig. 2. Computational domain with the number of radial and poloidal mesh points 36×96, fitting results of experimental data for L-mode shot 39090, and profiles of anomalous particle transport coefficient D and anomalous electron heat transport coefficient χ_e at the midplane from the fitting. The unit of the coordinates in the figure of "Physical mesh" is meter (m).

neutrals in the modelling. For neutrals, a Monte-Carlo treatment may be better. In the present modelling and fitting a fluid model is used for neutrals by using B2.5I. A dynamic Monte-Carlo treatment may be more reasonable for neutrals, but running the B2.5I with Eirene [10], which includes a dynamic Monte-Carlo treatment for neutrals, would enlarge the CPU time and produce noise in the results. The noise would make the judgement of convergence and the calculation of residuals by the code itself during the fitting more difficult. A good way for the dynamic Monte-Carlo treatment of neutrals can be considered by using the radial transport coefficients D, χ_e and χ_i from the B2.5I fitting, and running the coupling version B2.5–Eirene.

In order to get the modelling results for the validation assessment of the models in the coupling version of edge plasma transport code B2–Eirene, B2–Eirene has been used for modelling L-mode shot 24830 on JT-60U tokamak [11]. In the modelling the radial transport coefficients without spatial dependent were chosen, i.e. $D_\perp = 0.15\ \mathrm{m^2/s}$, $\chi_{e\perp} = \chi_{i\perp} = 5.0\ \mathrm{m^2/s}$. $D_\perp$ is similar to the anomalous particle transport coefficient D at $r - a = 0.0$ obtained from the present fitting of L-mode shot 39090 on JT-60U tokamak, but it is smaller than D when $r - a > 0.0$. $\chi_{e\perp}$ and $\chi_{i\perp}$ are, respectively, larger than χ_e and χ_i obtained from the present fitting of L-mode shot 39090. With the transport coefficients $D_\perp$, $\chi_{e\perp}$ and $\chi_{i\perp}$ the modelling results have been compared with the experimental data from L-mode shot 24830 [11]. At the midplane the good agreement between the experimental measurement and the B2–Eirene modelling result for the profile of the electron density can be found, but, the difference between the experimental measurement and the modelling result for the profile of the electron temperature also can be found. The difference may come from the usage of constant electron heat transport coefficient $\chi_{e\perp}$. From Fig. 1 in Ref. [11], the electron temperature at the midplane from the modelling result is higher than the experimental measurement in the SOL region far from the separatrix, in the region if $\chi_{e\perp}$ is set to the value smaller than $\chi_{e\perp} = 5.0\ \mathrm{m^2/s}$, the agreement between the experimental measurement and the modelling result may become better for the profile of electron temperature at the midplane. So, the radial transport coefficients with the radial dependent at a SOL plasma may be reasonable.

From the results in the present modelling and the previous modelling in Ref. [11] for L-mode shots, the difference between the modelling results and the experimental measurements is larger for the profiles of plasma parameter at the target plates of the divertor. There are some issues with the sheath and the radial electric field in the divertor modelling, also the flows and drifts are very important to get the divertor conditions right, so, not including these physics in the code might be the reason why there is no good match to the experimental measurement at the target plates of divertor. From the experimental measurements in L-mode shots 24830 and 39090, the H_α or D_α emission is inner/outer divertor asymmetry, but the modelling results for shots 39090 and 24830 tend to produce a more symmetric solution. So, the transport modelling in the divertor region is more difficult.

For H-mode shot 37856, the fitting results and the profiles of anomalous particle transport coefficient D and anomalous electron heat transport coefficient χ_e at the midplane are shown in Fig. 4.

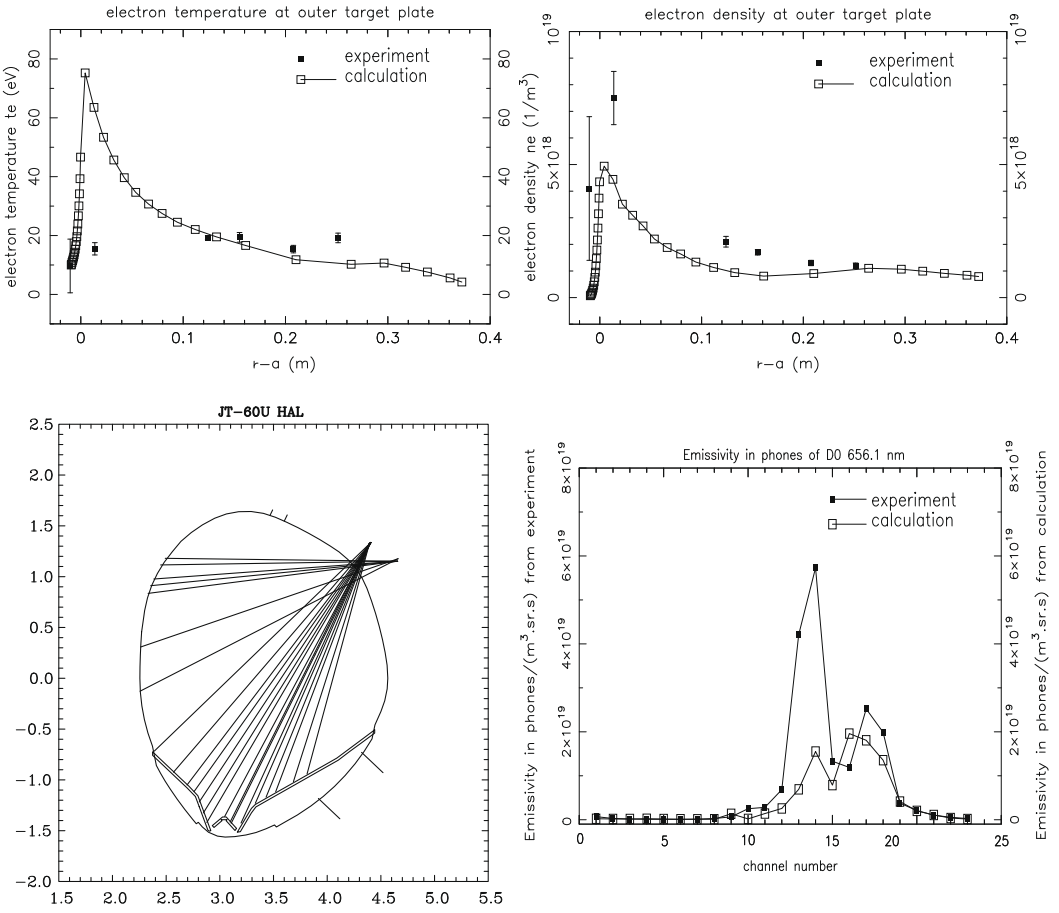

Fig. 3. Comparison between modelling results and the experimental data for the profiles of electron temperature and density at the outer target plate of the divertor and for the profile of D_α. The arrangement of 16 channels for D_α measurement is also shown in the figure with the unit of the coordinates meter (m), the channel number decreases clockwise.

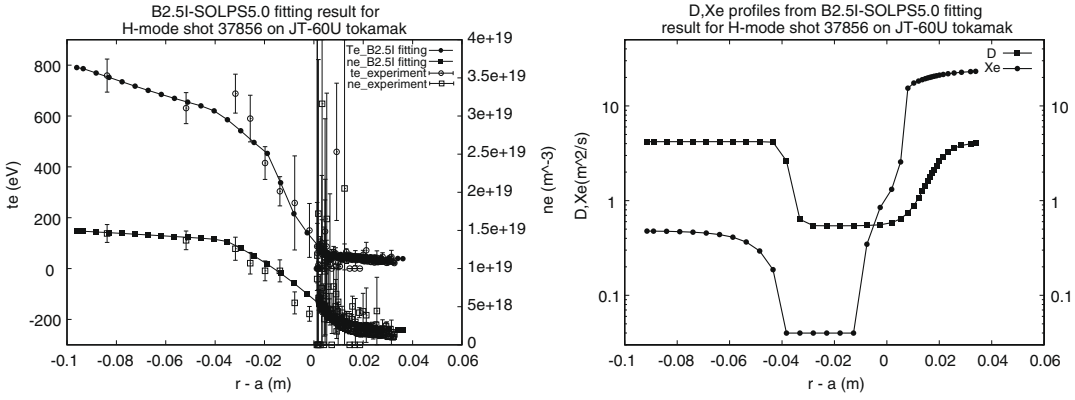

Fig. 4. Fitting results of experimental data for H-mode shot 37856, profiles of anomalous particle transport coefficient D and anomalous electron heat transport coefficient χ_e at the midplane from the fitting.

Because the profile of ion temperature is also not available in the computational region for the shot, it is again assumed that the anomalous ion heat transport coefficient χ_i and anomalous electron heat coefficient χ_e are equal.

The fitting results show that the anomalous transport coefficients D and χ_e have large drop within the Edge Transport Barrier (ETB) in the H-mode shot 37856, which confirms the results obtained before by other authors [12], namely that microturbulence is suppressed within the ETB in H-mode shots and the anomalous transport coefficients may drop to neoclassic level, but, what kind of microturbulence is suppressed is under discussion.

For H-mode shot 37856, the good match of the modelling results to the profiles of plasma parameters at the target plates of divertor has not been found. With the transport coefficients D, χ_e and χ_i from the fitting, Fig. 5 shows the profiles of electron temperature and density at the outer target plate of divertor. In the figure, 'Rpos' is the radial position from the center of the machine. It is very difficult to get good match results for the profiles of plasma parameter at divertor before some physics models, for example, the drifts, are included in the transport code. The more work should be done for matching the code results to the experimental measurements in the diveror region.

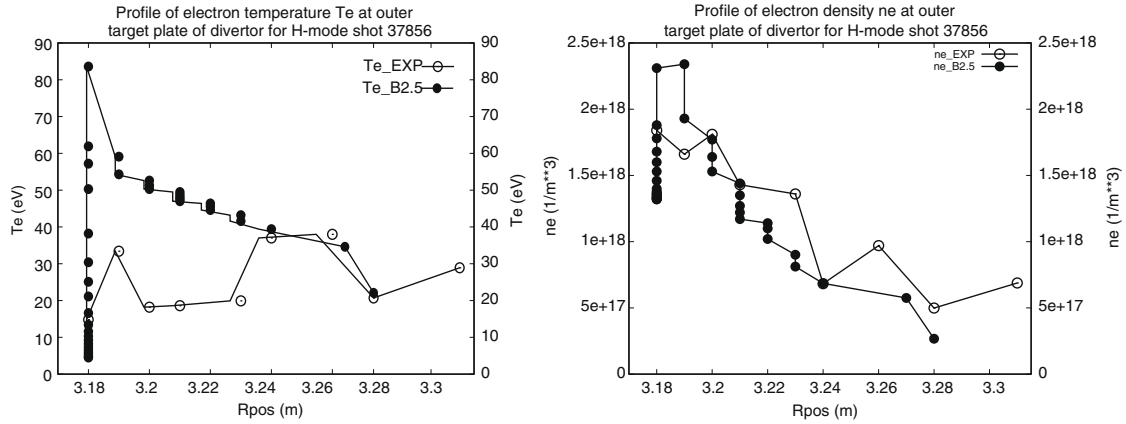

Fig. 5. Profiles of electron temperature and density at the outer target plate of divertor for H-mode shot 37856 with the transport coefficients D, χ_e and χ_i from the fitting.

For the Type I ELMy H-mode shots 17151 and 17396 on ASDEX Upgrade [13] and for Type III ELMy H-mode shot on TCV [14] the measured profiles of plasma parameters at the midplane also have been matched by the full B2–Eirene modelling results for the transport analysis and the radial transport coefficients D, χ_e have been obtained. The modelling and match results also showed the anomalous transport coefficients D and χ_e have large drop within the Edge Transport Barriers (ETBs). The edge plasma transport code EDGE2D was used for modelling Type I ELMy H-mode shot 58569 on JET and matching the modelling results to the experimental temperature and density profiles by varying the perpendicular heat conductivities $\chi_{e,i}$ and the particle transport coefficient D in the code, a good agreement between the code results and the measurement data is obtained by using D and χ_e with three different plateau values, respectively, for three different regions and the assumption of $\chi_i = \chi_e$ [15]. From Fig. 2 in Ref. [15] for JET shot 58569, after dropping to lower value within the ETB $\chi_{e,i}$ increase again and reach to 1 m^2/s. The profiles of radial transport coefficients from H-mode shots on ASDEX Upgrade, JET and TCV are very similar to the profiles of D and χ_e obtained from the present fitting results of H-mode shot 37856 on JT-60U tokamak.

3. Summary

The profiles of anomalous particle transport coefficient D, anomalous electron and ion heat transport coefficients χ_e, χ_i have been obtained by modelling plasma experiments and fitting the experimental data from L-mode shot 39090 and H-mode shot 37856 in JT-60U tokamak with NBI and ohmic heating. The anomalous transport coefficients D, χ_e and χ_i from the fitting have a radial dependence and they consist of qualitatively different parts. From the experimental results, it can be seen that in H-mode shot 37856 steep gradients and pedestals near the separatrix have been formed in the plasma parameter profiles. From the modelling and fitting results at the pedestal region, the anomalous transport coefficients D and χ_e show larger drops compared with the anomalous transport coefficients at other sections in the profiles. For L-mode shot 39090, D and χ_e obtained from the fitting increase radially. Because the modelling and fitting results for L-mode shot 39090 do not go far enough inside the separatrix, it is difficult to get information about the anomalous transport coefficients near the separatrix.

Significant difference between the modelling results and the experimental measurements have been found for the profiles of plasma parameters at the outer target plates in both L-mode shot 39090 and H-mode shot 37856. In order to improve the modelling and fitting results, in the next step, B2.5–Eirene will be used for modelling experimental shots from JT-60U tokamak, and impurities and drifts will be taken into account.

Acknowledgements

This work was supported by National Natural Science Foundation of China (No. 10275066) and was partly supported by the JSPS-CAS Core-University Program on Plasma and Nuclear Fusion. This work also was supported by Center for Computational Science, Hefei Institutes of Physical Sciences. The authors greatly appreciate Max-Planck-Institut für Plasmaphysik in Garching for providing the SOLPS5.0 code package.

References

[1] R. Schneider, X. Bonnin, K. Borrass, D.P. Coster, H. Kastelewicz, D. Reiter, V.A. Rozhansky, B.J. Braams, Contribution Plasma Phys. 46 (1&2) (2006) 3.
[2] D.P. Coster, X. Bonnin, et al., J. Nucl. Mater. 337–339 (2005) 366.
[3] B. Braams et al., Contribution Plasma Phys. 36 (1996) 276.
[4] V.A. Rozhansky, S.P. Voskoboynikov, E.G. Kaveeva, D.P. Coster, R. Schneider, Nucl. Fus. 41 (4) (2001) 387.
[5] D.P. Coster, J.W. Kim, G. Haas, B. Kurzan, H. Murmann, J. Neuhauser, H. Salzmann, R. Schneider, W. Schneider, J. Schweinzer, ASDEX Upgrade Team, Contribution Plasma Phys. 40 (3&4) (2000) 334 (Proceedings of the Seventh PET Conference, Tajimi, Gifu, Japan, 4–6 October, 1999).
[6] J.-W. Kim, D.P. Coster, J. Neuhauser, R.Schneider, ASDEX Upgrade Team, J. Nucl. Mater. 290–293 (2001) 644 (Proceedings of the 14th PSI, Rosenheim, Germany, 22–26 May 2000).
[7] H. Takenaga, JT-60 Team, Nucl. Fus. 47 (2007) S563.
[8] H. Kawashima, K. Shimizu, T. Takizuka, N. Asakura, H. Takenaga, T. Nakano, S. Sakurai, J. Nucl. Mater. 363–365 (2007) 786.
[9] N. Asakura, H. Takenaga, S. Sakurai, G.D. Porter, T.D. Rognlien, M.E. Rensink, K. Shimizu, S. Higashijima, H. Kubo, Nucl. Fus. 44 (2004) 503.
[10] D. Reiter et al., J. Nucl. Mater. 196–198 (1992) 80.
[11] A. Loarte et al., J. Nucl. Mater. 266–269 (1999) 1123.
[12] V.V. Parail, Plasma Phys. Control. Fus. 44 (2002) A63.
[13] L.D. Horton, A.V. Chankin, Y.P. Chen, et al., Nucl. Fus. 45 (2005) 856.
[14] B. Gulejová et al., J. Nucl. Mater. 363–365 (2007) 1037.
[15] A. Kallenbach, Y. Andrew, M. Beurskens, G. Corrigan, T. Eichl, et al., Plasma Phys. Control. Fus. 46 (2004) 431.